ACS OMEGA

Open Access

http://pubs.acs.org/journal/acsodf

Article

Engineering Three-Dimensional Spheroid Culture for Enrichment of Proangiogenic miRNAs in Umbilical Cord Mesenchymal Stem Cells and Promotion of Angiogenesis

Ramya Lakshmi Rajendran, Prakash Gangadaran, Ji Min Oh, Chae Moon Hong, and Byeong-Cheol Ahn*

Cite This: *ACS Omega* 2024, 9, 40358−40367

Read Online

ACCESS | Metrics & More | Article Recommendations | Supporting Information

ABSTRACT: In the field of regenerative medicine, umbilical cord-derived mesenchymal stem cells (UC-MSCs) have a plausible potential. However, traditional two-dimensional (2D) culture systems remain limited in replicating the complex *in vivo* microenvironment. Thus, three-dimensional (3D) cultures offer a more physiologically relevant model. This study explored the impact of 3D culture conditions on the UC-MSC secretome and its ability to promote angiogenesis, both *in vitro* and *in vivo*. In this study, using two distinct methods, we successfully cultured UC-MSCs: in a monolayer (2D-UC-MSCs) and as spheroids formed in U-shaped 96-well plates (3D-UC-MSCs). The presence and expression of proangiogenic miRNAs in the conditioned media (CM) of these cultures were investigated, and differential expression patterns were explored. Particularly, the CM of 3D-UC-MSCs revealed significantly higher levels of miR-21-5p, miR-126-5p, and miR-130a-3p compared to 2D-UC-MSCs. Moreover, the CM from 3D-UC-MSCs revealed a higher effect on endothelial cell proliferation, migration, and tube formation than did the CM from 2D-UC-MSCs, indicating their proangiogenic potential. In an *in vivo* Matrigel plug mouse model, 3D-UC-MSCs (cells) stimulated greater vascular formation compared to 2D-UC-MSCs (cells). 3D culture of UC-MSCs' secretome improves the promotion of angiogenesis.

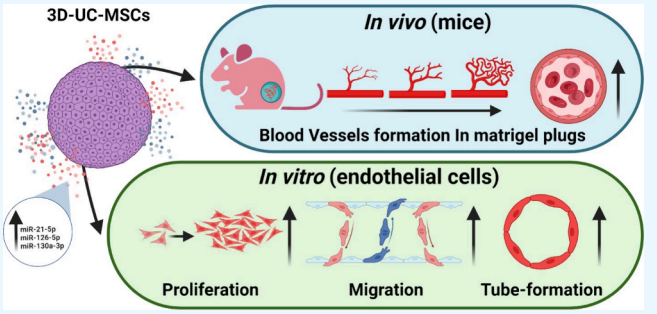

1. INTRODUCTION

In recent years, regenerative medicine has witnessed astounding advancements, highlighting harnessing the therapeutic potential of mesenchymal stem cells (MSCs) to address various clinical challenges. The human umbilical cord has gained considerable attention owing to its unique advantages, including noninvasive procurement, higher proliferative capacity, and low immunogenicity among the diverse sources of MSCs.[1−3] MSCs derived from the umbilical cord (UC-MSCs) have exhibited an immense potential for tissue repair and regeneration. Their ability to secrete a wide array of paracrine factors, collectively known as the "secretome", has been identified as a key contributor to their therapeutic effects.[4−6]

While conventional two-dimensional (2D) culture systems have provided valuable insights into UC-MSC's biology and regenerative potential, these platforms do not fully reproduce the native three-dimensional (3D) microenvironment[7,8] in which these UC-MSCs naturally reside within the umbilical cord and the surrounding tissue.[9] Thus, growing interest exists in exploring the impact of 3D culture systems on UC-MSC behavior, particularly concerning their secretome and angiogenic potential. By providing a more physiologically relevant microenvironment, we hypothesized that 3D cultures may enhance the therapeutic properties of UC-MSCs, ultimately improving their clinical utilities.[10,11]

The secretome of UC-MSCs involves a complex mixture of growth factors, cytokines, chemokines, nucleic acids, and extracellular vesicles (EVs), which collectively mount a range of cellular processes, including inflammation modulation, immunomodulation, and tissue repair.[11−15] These paracrine factors are known to exert proangiogenic effects, thus making UC-MSCs a promising cell source for angiogenesis-promoting therapies in conditions such as ischemic diseases, wound healing, and tissue engineering.[16]

In this context, the present study aims to explore the profound influence of 3D culture systems on UC-MSCs and conditioned media (CM) (exclusively angiogenic miRNAs),

Received: March 1, 2024
Revised: July 30, 2024
Accepted: August 14, 2024
Published: September 20, 2024

particularly emphasizing their capacity for angiogenesis promotion. The CM of UC-MSCs was tested regarding the capacity of CMs from 2D-UC-MSCs and 3D-UC-MSCs to promote angiogenesis on endothelial cells *in vitro*. Moreover, the transition from *in vitro* experiments to *in vivo* models will allow us to evaluate the translational potential of 3D-cultured UC-MSCs in real-life scenarios, becoming a springboard for future clinical applications. Therefore, the angiogenic effects of 2D-UC-MSCs and 3D-UC-MSCs were tested on an angiogenic *in vivo* mouse model.

2. MATERIALS AND METHODS

2.1. Cell Lines. UC-MSCs were obtained from the American Type Culture Collection (ATCC) (Manassas, VA). UC-MSCs were cultured in Dulbecco's modified Eagle's (DMEM)-F12 medium (HyClone, Logan, UT). Mouse endothelial cells (SVEC4−10) were acquired from ATCC and cultured in DMEM high-glucose (HyClone). The medium was supplemented with 10% fetal bovine serum (FBS; Hyclone) and antibiotics (1% penicillin−streptomycin) (Gibco, Carlsbad, CA) and maintained at 37 °C in a 5% CO_2 atmosphere.

2.2. Monolayer (2D) or Spheroid (3D) Cell Cultures. For adherent 2D monolayer cultures, standard cell culture (100 mm) plates were used. For 3D spheroid cell cultures, U-shaped 96-well culture plates were used. Cells (10,000) in 200 μL of medium were seeded into U-shaped 96-well plates (SPL Life Sciences, Gyeonggi-do, Republic of Korea) and grown until day 5. Cells/spheroids formation was assessed using an AXIO microscope (Zeiss, Baden-Württemberg, Germany), and the size of the spheroids were measured using ZEN 2.3 (blue edition) software (Zeiss, Oberkochen, Germany).

2.3. Cellular Proliferation of 2D-UC-MSCs and 3D-UC-MSCs. Cells (10,000) in 200 μL of medium were seeded into flat surface 96-well plates or U-shaped 96-well plates (SPL Life Sciences, Gyeonggi-do, Republic of Korea) and maintained for 5 days at 37 °C in a 5% CO_2. A CCK8 assay kit (Dojindo Molecular Technologies, Kyushu, Japan) was used to evaluate cell proliferation. A CCK8 reagent (20 μL) was added to the wells and maintained for 2 h at 37 °C in a 5% CO_2 incubator according to the manufacturer's protocol.

2.4. Western Blotting Analysis. Western blot analysis was conducted on fibroblasts/DP cells/nanovesicles with lysates prepared using RIPA buffer (Thermo Fisher Scientific, Waltham, MA). Equal amounts of samples were loaded and separated via 10% sodium dodecyl sulfate-polyacrylamide gel electrophoresis and then transferred onto PVDF membranes (Millipore, Burlington, MA). The membranes were probed with primary antibodies (CD133 and CD166 from Abcam), followed by secondary antibodies conjugated with horseradish peroxidase (Cell Signaling Technology, Danvers, MA). Signal detection was performed using enhanced chemiluminescence (GE Healthcare, Chicago, IL), as per the manufacturer's instructions. The signals were visualized using a Fusion FX chemiluminescence analyzer system (Vilber Lourmat, Marnela-Vallée, France). The images were cropped and prepared using Microsoft PowerPoint (Microsoft, Redmond, WA). The blots were stained with Ponceau S staining, which was used as a loading control. The intensity was measured by using GelQuant. NET software (version 1.8.2) (Biochem Lab Solutions).

2.5. Quantitative Real-Time Polymerase Chain Reaction (qRT-PCR). Using the TRIzol reagent method, total RNA was extracted from both 2D-UC-MSCs and 3D-UC-MSCs. Subsequently, cDNA conversion was performed using the High-Capacity cDNA Reverse Transcription Kit (Thermo Fisher Scientific) according to the manufacturer's instructions. The mRNA expression of genes was detected using a qRT-PCR analysis and performed with SsoAdvanced Universal SYBR Green Supermix reagent (Bio-Rad Laboratories, Hercules, CA) on a CFX96 Touch Real-Time PCR Detection System (Bio-Rad Laboratories) according to the manufacturer's instructions. The sense and antisense primers are listed in Supplementary Table S1. The mRNA expression data were expressed in fold change, and the expression between 2D-UC-MSCs and 3D-UC-MSCs was calculated using the $2^{-\Delta\Delta Ct}$ method.[17]

2.6. Preparation of CM. 2D-UC-MSCs and 3D-UC-MSCs were cultured as described above. The CMs (2D-UC-MSC-CMs and 3D-UC-MSC-CMs) were collected, centrifuged at 415 g for 5 min, and then filtered through a 0.22 μm syringe filter; CMs were concentrated using protein concentrators PES, 3K MWCO (Thermo Fisher Scientific). Using a BCA protein assay kit (Thermo Fisher Scientific), the CM protein content was measured.

2.7. TaqMan Assay. Using the TRIzol reagent method, total RNA was extracted from both the CM of 2D-UC-MSCs and 3D-UC-MSCs. Subsequently, cDNA conversion was performed using the TaqMan Advanced miRNA cDNA Synthesis Kit (Thermo Fisher Scientific) according to the manufacturer's instructions. The miRNA expression levels in 2D-UC-MSCs and 3D-UC-MSCs were assessed via qRT-PCR, employing TaqMan Advanced miRNA Assays and the ABI-7500 detection system (Applied Biosystems, United States), following the manufacturer's guidelines. Specifically, using TaqMan Advanced miRNA Assays, miR-21-5p, miR-126-5p, miR-130a-3p, miR-204-5p, miR-210-3p, and miR-494-5p were quantified as well as miR-20a-5p, which was utilized as a normalizing control. The miRNA expression data were expressed in fold change, and the expression between CM of 2D-UC-MSCs and 3D-UC-MSCs was calculated using the $2^{-\Delta\Delta Ct}$ method.[17]

2.8. Cellular Proliferation Assay. Briefly, 2×10^4 SVEC4 cells were seeded in 100 μL of complete medium in 96-well plates and incubated for 24 h with 2D-UC-MSC-CMs (0, 2, 4, 6, 8, and 10 μg/μL) or 3D-UC-MSC-CMs (0, 2, 4, 6, 8, and 10 μg/μL) at 37 °C in a 5% CO_2 atmosphere. A CCK8 assay kit (Dojindo Molecular Technologies, Kyushu, Japan) was used to evaluate cell proliferation. A CCK8 reagent (10 μL) was added to the wells and maintained for 2 h at 37 °C in a 5% CO_2 incubator according to the manufacturer's protocol.

2.9. Transwell Migration Assay. In 200 μL of medium, a total of 5×10^4 SVEC4 cells were suspended and placed on the Transwell membrane. In the lower chamber, 600 μL of medium containing 3% FBS was added. Simultaneously, 8 μg/mL 2D-UC-MSC-CMs and 3D-UC-MSC-CMs were applied to the top of the inset, and the setup was placed in a CO_2 incubator for a 24 h incubation period. Thereafter, using the crystal violet staining method, the cells were fixed and stained, as previously described.[18] Observation and imaging were conducted using a Nikon Eclipse Ti Fluorescence Microscope (Nikon Corp., Tokyo, Japan).

2.10. Matrigel Tube Formation Assay. Matrigel (200 μL) was added to a 48-well plate and maintained at 37 °C and 5% CO_2 for 2 h. Next, 5×10^4 SVEC4 containing 8 μg/mL 2D-UC-MSC-CMs and 3D-UC-MSC-CMs in 200 μL of

https://doi.org/10.1021/acsomega.4c02037
ACS Omega 2024, 9, 40358−40367

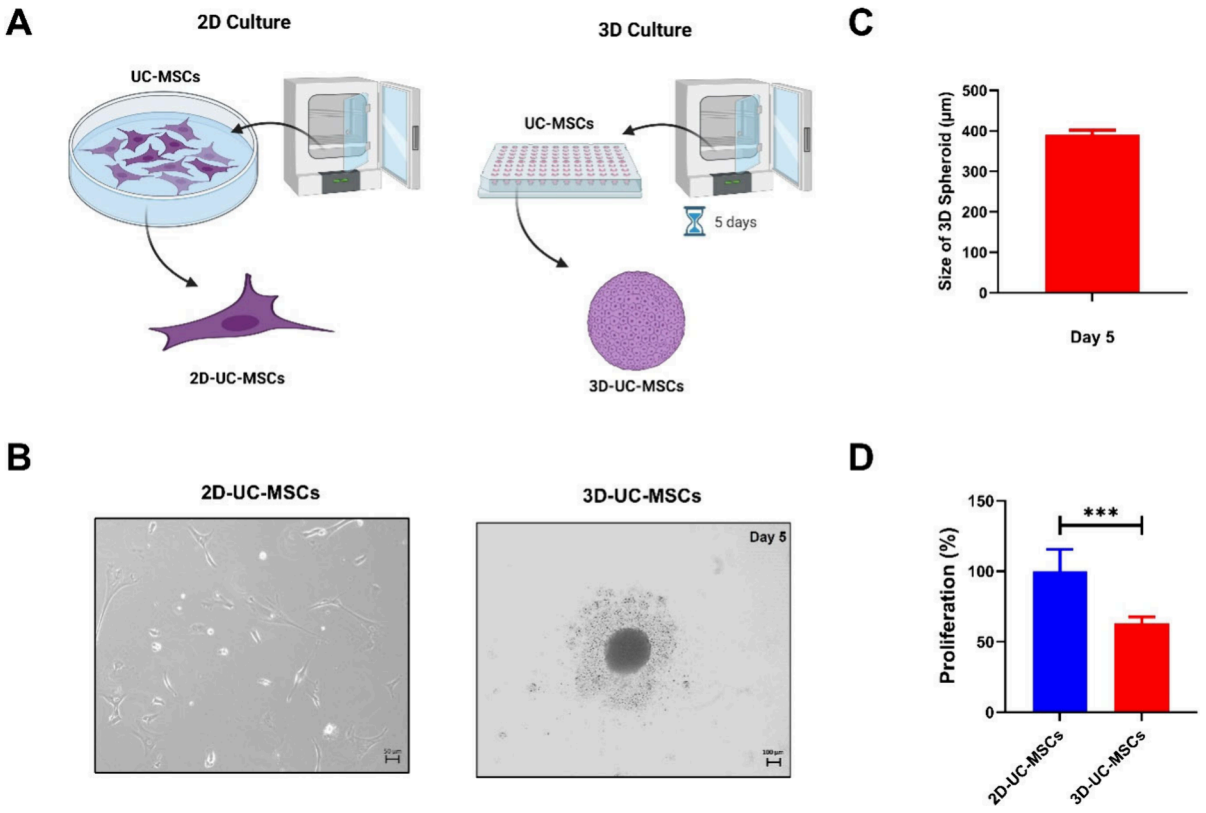

Figure 1. Monolayer (2D) or spheroid (3D) cell cultures of umbilical cord-derived mesenchymal stem cells (UC-MSCs). (A) Graphical illustration of cultures of monolayer (2D) or spheroid (3D) cell cultures of UC-MSCs, created using BioRender.com. (B) UC-MSCs in monolayer (2D-UC-MSCs) (scale bar: 50 μm) and formation of spheroids from day U-shaped 96-well plates (3D-UC-MSCs); the spheroids were grown until day 5 (scale bar: 100 μm). (C) Average size of the 3D spheroid at day 5 (n = 4). (D) 2D-UC-MSCs and 3D-UC-MSCs' cell proliferation quantified using a CCK8 assay on day 5 (n = 4). Statistical significance is denoted as follows: ***p < 0.001, as determined by the Student's t test.

medium were added to each well and incubated at 37 °C and 5% CO_2 for 4 h. After 4 h of treatment, tube formation was assessed using an AXIO microscope (Zeiss, Baden-Württemberg, Germany). The vessel parameters were automatically measured using the AngioTool software (National Cancer Institute, Radiation Oncology Branch, Angiogenesis Core Facility, MD, United States).[19]

2.11. *In Vivo* Experiments and Histology. Pathogen-free, 6-week-old male Balb/c nude mice were purchased from Hana, Busan, Republic of Korea. Mice were maintained under specific pathogen-free conditions and allowed to acclimate to the environment for 1 week prior to the initiation of the experiments.

Animal experiments and all procedures were reviewed and approved by Kyungpook National University's Animal Care and Use Committee (IRB NO: KNU-2023−0237). All experiments were performed in accordance with relevant guidelines and regulations and executed in compliance with the guiding principles for the Care and Use of Laboratory Animals and the ARRIVE guidelines (https://arriveguidelines.org).

The mice were anesthetized with 2.5% Isoflurane (Hana Pharma, Co., Ltd., Kyonggi-Do, Republic of Korea), and a subcutaneous injection was administered into the right lower flank to start the experiments. Mice were then divided into three groups: the Matrigel-only group (n = 6) received 300 μL of Matrigel, the 2D-UC-MSC group (n = 6) received 300 μL of Matrigel with 0.5 × 10^6 2D-UC-MSCs, and the 3D-UC-MSCs group (n = 6) received 300 μL of Matrigel with 0.5 × 10^6 3D-UC-MSCs. The Matrigel plugs were extracted after a 2 week period, and images were captured using a surgical microscope (M320 F12; Leica Microsystems, Germany). The Matrigel plugs were immediately fixed in 10% neutral buffered formalin after imaging, embedded in paraffin, and sliced into 3−4 μm sections. These sections were stained with hematoxylin and eosin (H&E) and visualized under an AXIO microscope (Zeiss, Oberkochen, Germany). Thereafter, the areas of all blood vessels were quantified using ZEN 2.3 (blue edition) software (Zeiss, Oberkochen, Germany).

2.12. Statistical Analysis. All data are expressed as the mean ± standard deviation. The differences between pairs of groups were analyzed using a student's t test in Excel (Microsoft) or GraphPad Prism 9.4.1.681 (GraphPad Software Inc., San Diego, CA, United States). Statistical significance was set at p < 0.05.

3. RESULTS

3.1. Successful Culture of UC-MSCs in (2D) Monolayer or (3D) Spheroids. Using two different methods, UC-MSCs were cultured in a monolayer (referred to as 2D-UC-MSCs) and as spheroids formed in U-shaped 96-well plates (referred to as 3D-UC-MSCs) (Figure 1A). In 2D-UC-MSCs, the cells were grown in a flat, single layer, as shown in Figure 1B, left panel. Conversely, for 3D-UC-MSCs, the cells were seeded into specially designed U-shaped 96-well plates, encouraging cell aggregation into compact spherical structures known as spheroids, and cells were grown until day 5 (Figure 1B, right panel). The results suggest that on day 5 of the experiment, the average size of the 3D spheroids was approximately 390.1 ±

https://doi.org/10.1021/acsomega.4c02037
ACS Omega 2024, 9, 40358−40367

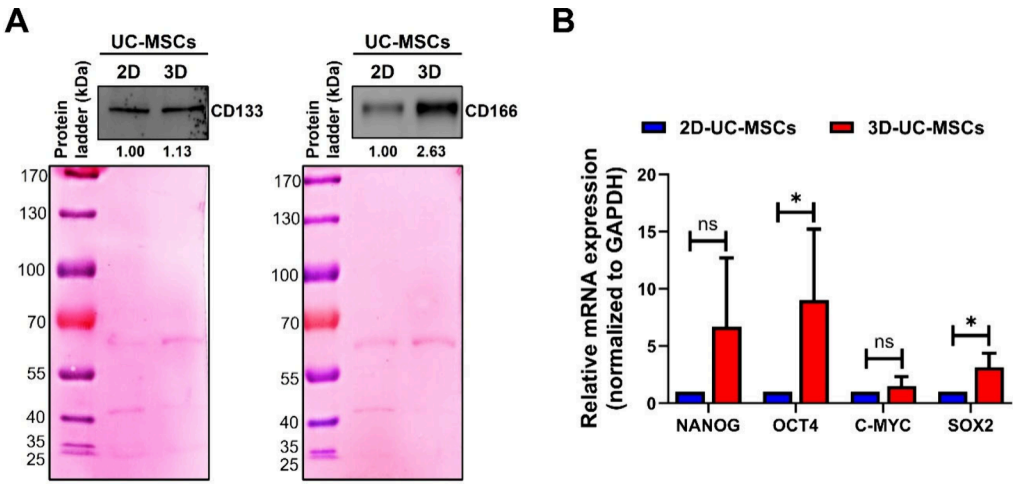

Figure 2. Spheroid (3D) cell cultures increased the stemness of UC-MSCs. (A) Western blot analysis of CD133 and CD166 levels in 2D-UC-MSCs and 3D-UC-MSCs (day 5), with Ponceau S staining used as loading control. (B) qRT-PCR results of mRNA expressions of *NANOG*, *OCT4*, *C-MYC*, *SOX2*, and *GAPDH* in 2D-UC-MSCs and 3D-UC-MSCs (day 5) (n = 3). Statistical significance is denoted as follows: *p < 0.05; ns, not significant as determined by the Student's t test.

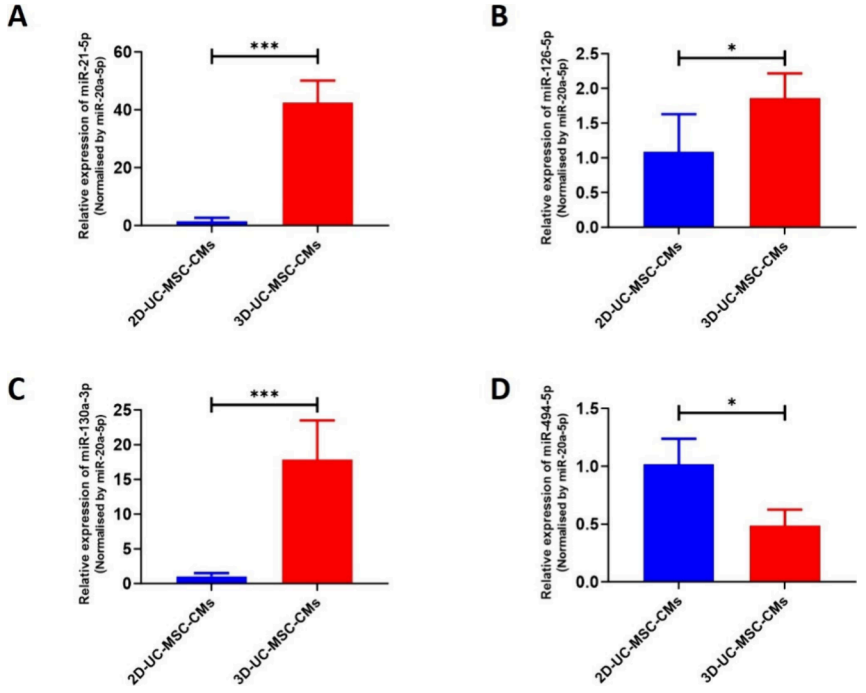

Figure 3. Angiogenic miRNA expression in conditioned media of 2D-UC-MSCs and 3D-UC-MSCs. (A–D) The expression of miRNAs (miR-21-5p, miR-126-5p, miR-130a-3p, and miR-494-5p) in 2D-UC-MSC-CMs and 3D-UC-MSC-CMs (n = 3) and miR-20a-5p used as loading control; bar graph of the fold change of 3D-UC-MSC-CMs/2D-UC-MSC-CMs. Statistical significance is denoted as follows: *p < 0.05 and ***p < 0.001, as determined by the Student's t test.

11.9 μm (Figure 1C). Cellular proliferation of 2D-UC-MSCs was significantly (p < 0.001) higher than 3D-UC-MSCs (Figure 1D). The Western blot result showed that stem cell markers such as CD133 (1.13-fold) and CD166 (2.63-fold) were increased in 3D-UC-MSCs compared to 2D-UC-MSCs (Figure 2A). Furthermore, the mRNA expression levels of stemness markers such as *NANOG*, *OCT4*, *C-MYC*, and *SOX2* were analyzed on 2D-UC-MSCs and 3D-UC-MSCs; qRT-PCR results revealed that *NANOG* was substantially (p = 0.08) increased in 3D-UC-MSCs than 2D-UC-MSCs, *OCT4* and *SOX2* were significantly (p < 0.05) increased in 3D-UC-MSCs than 2D-UC-MSCs, *C-MYC* was not significantly increased (p > 0.05) but slightly increased in 3D-UC-MSCs than 2D-UC-MSCs (Figure 2B). These findings strongly suggest that a scaffold-free 3D culture of UC-MSCs was successful.

3.2. Detection and Expression of Angiogenic miRNAs in CM of 2D-UC-MSCs and 3D-UC-MSCs. The presence of known proangiogenic miRNAs, including miR-21-5p, miR-126-5p, miR-130a-3p, miR-204-5p, miR-210-3p, and miR-494-5p, in both 2D-UC-MSC-CMs and 3D-UC-MSC-CMs was examined. Our results verified the presence of all six miRNAs in 3D-UC-MSC-CMs and four in 2D-UC-MSC-CMs. Strikingly, miR-21-5p demonstrated a significantly higher expression (p < 0.001) in 3D-UC-MSC-CMs compared to

https://doi.org/10.1021/acsomega.4c02037
ACS Omega 2024, 9, 40358−40367

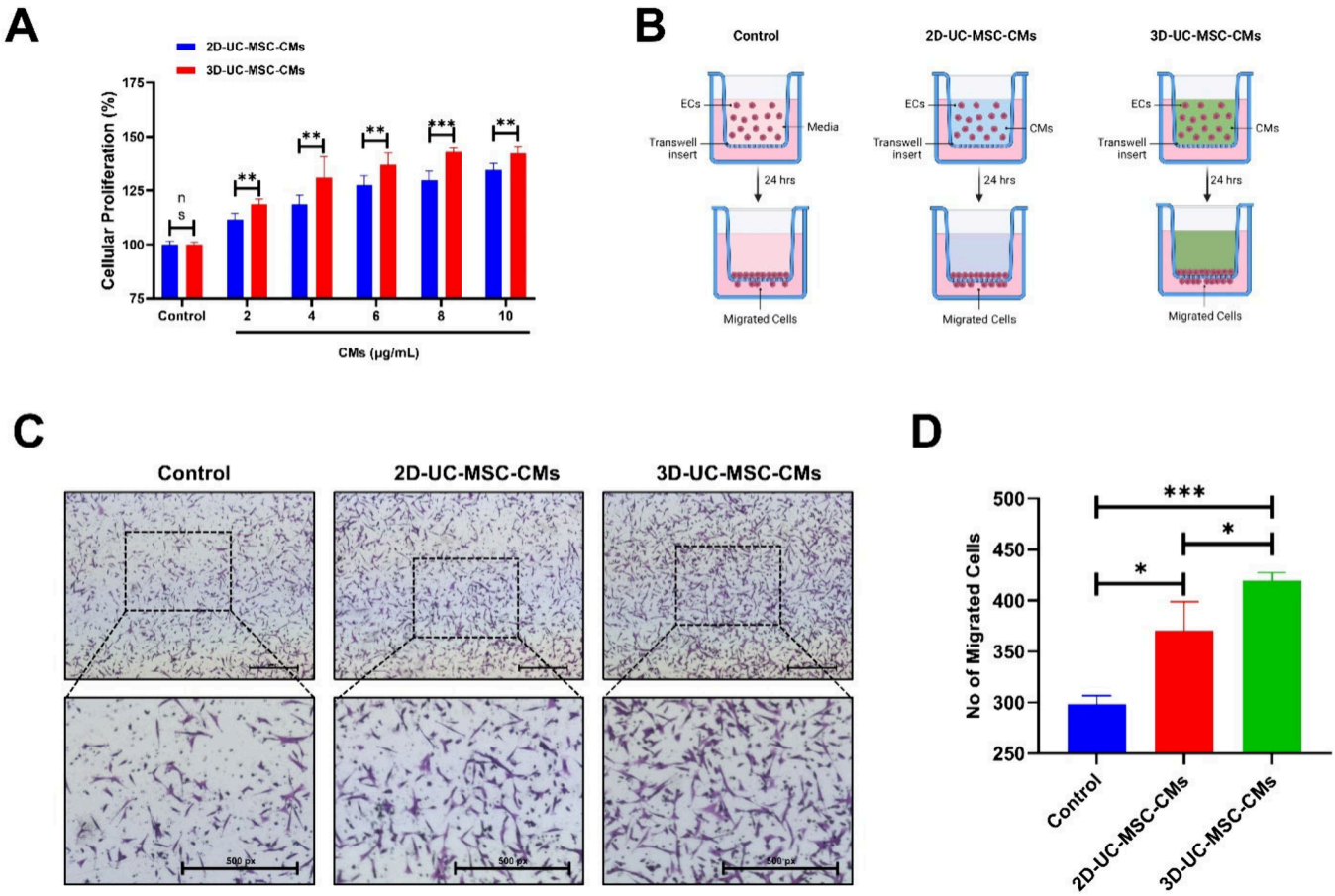

Figure 4. Endothelial cell proliferation and migration after treatment with CMs of 2D-UC-MSCs and 3D-UC-MSCs. (A) Endothelial cell proliferation quantified using a CCK8 assay, after a 24-h treatment with 2D-UC-MSC-CMs/3D-UC-MSC-CMs (0, 2, 4, 6, 8, and 10 μg/μL) (n = 5). (B) An illustrative diagram of the migration assay (created using BioRender.com). (C) Phase-contrast microscopy images depicting endothelial cell migration following a 24 h treatment with 8 μg/mL of 2D-UC-MSCs/3D-UC-MSCs. (D) Quantification of the number of migrated cells in (C) (n = 3). Statistical significance is denoted as follows: *p < 0.05, **p < 0.01, and ***p < 0.001, as determined by the Student's t test.

2D-UC-MSC-CMs, with an approximately 42-fold increase (Figure 3A). Similarly, miR-126-5p displayed a considerably higher expression (p < 0.05) in 3D-UC-MSC-CMs compared to 2D-UC-MSC-CMs, with an approximately 1.9-fold increase (Figure 3B). MiR-130a-3p also showed a significantly higher expression (p < 0.001) in 3D-UC-MSC-CMs compared to 2D-UC-MSC-CMs, with an approximately 17.8-fold increase (Figure 3C). Conversely, miR-494-5p was remarkably lower (p < 0.05) in 3D-UC-MSC-CMs than in 2D-UC-MSC-CMs (Figure 3D). Notably, miR-204-5p and miR-210-3p were exclusively detected in 3D-UC-MSC-CMs and were absent in 2D-UC-MSC-CMs. The average cycle threshold (C_t) value for miR-204-5p was 29.2, signifying the presence of ample target nucleic acids within the 3D-UC-MSC-CMs. The average C_t value of miR-210-3p was 38.1, indicative of the limited quantities of target nucleic acids in 3D-UC-MSC-CMs (Figure S1). These results conclusively confirm the presence of various proangiogenic miRNAs in 3D-UC-MSC-CMs and underscore that some are more abundant than their 2D counterparts.

3.3. CMs of 3D-UC-MSCs Induced Endothelial Cell Proliferation and Migration. Both 2D-UC-MSC-CM and 3D-UC-MSC-CM treatments led to an increase in the proliferation of endothelial cells. Remarkably, treatment with 3D-UC-MSC-CM demonstrated a significantly higher level of cell proliferation compared to 2D-UC-MSC-CMs, with statistical significance observed at concentrations of 2−6 μg/mL (p < 0.01), 8 μg/mL (p < 0.001), and 10 μg/mL (p < 0.01) (Figure 4A). CMs at a concentration of 8 μg/mL from both 2D-UC-MSCs and 3D-UC-MSCs were employed for further experiments. The study examined the ability of 3D-UC-MSC-CMs and 3D-UC-MSC-CMs to promote endothelial cell movement (Figure 4B). The transwell migration assay results indicated that both 2D-UC-MSC-CMs (p < 0.05) and 3D-UC-MSC-CMs (p < 0.001) significantly enhanced endothelial cell migration compared to the control. Additionally, 3D-UC-MSC-CM treatment showed a significantly higher level of cell migration when compared to 2D-UC-MSC-CMs (p < 0.05) (Figure 4C,D).

3.4. CMs of 3D-UC-MSCs induced endothelial cell tube formation. Fresh blood vessel development by endothelial cells reflects a critical facet of angiogenesis. We conducted an *in vitro* tube formation assay to evaluate the impact of CMs of 2D-UC-MSCs and 3D-UC-MSCs on endothelial cells in a Matrigel (Figure 5A). Our findings showed that 3D-UC-MSC-CMs significantly increased the total vessel length percentage (p < 0.05), while 2D-UC-MSC-CMs exhibited a notable increase in the same parameter compared to the control (Figure 5B). 3D-UC-MSC-CMs significantly increased the total number of junction percentage (p < 0.05), and 2D-UC-MSC-CMs displayed a similar effect compared to the control (Figure 5C). 3D-UC-MSC-CMs significantly increased the junction density percentage (p <

https://doi.org/10.1021/acsomega.4c02037
ACS Omega 2024, 9, 40358−40367

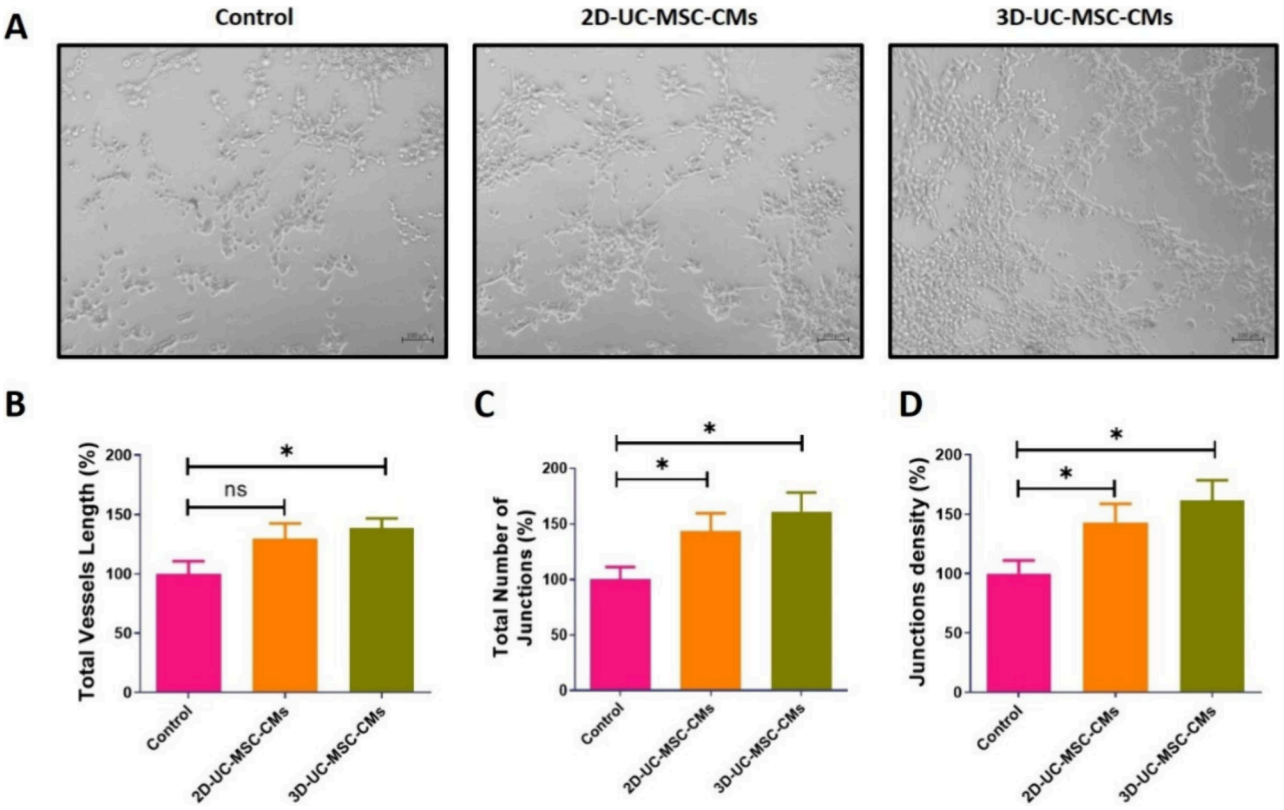

Figure 5. Endothelial cell tube formation after treatment with CMs of 2D-UC-MSCs and 3D-UC-MSCs. (A) The representative phase-contrast images of endothelial cells cultured on Matrigel-coated plates in medium treatment with 8 μg/mL of 2D-UC-MSCs/3D-UC-MSCs (scale bar: 100 μm). (B−D) Using AngioTool64 software, version 0.6a (02.18.14), the relative percentage of total vessel length, number of junctions, and junction density were quantified in the images (n = 3). Statistical significance is designated as follows: *p < 0.05; ns, not significant as determined by the Student's t test.

0.05), while 2D-UC-MSC-CMs revealed a similar increase compared to the control (Figure 5D). 3D-UC-MSC-CM administration had a markedly greater influence on all of the parameters (Figure 5B−D). These results indicate the potential therapeutic benefits of using CMs from 3D-cultured UC-MSCs for angiogenesis promotion.

3.5. 3D-UC-MSC treatment increased the number of vascular formations in a Matrigel plug mouse model. A schematic representation of the *in vivo* Matrigel plug mouse model is illustrated in Figure 6A. The experiment was stratified into three groups: one receiving Matrigel alone (control), another with Matrigel combined with 2D-UC-MSCs, and the third with Matrigel combined with 3D-UC-MSCs. These mixtures were injected under the skin of the mice. After a 14 day period, we extracted the Matrigel plugs for analysis. It was evident that the Matrigel-only group showed no visible new blood vessel formation on visual inspection. In contrast, the other two groups exhibited observable blood and blood vessels, as suggested by the presence of red blood cells in red color (Figure 6B, upper panel). H&E staining of cross sections of the plugs further verified the presence of blood vessels. Notably, large blood vessels (as indicated by yellow arrows) are visible in the H&E-stained sections of the 3D-UC-MSC group compared to both the 2D-UC-MSCs and control groups (Figure 6B, middle and lower panels). In terms of the blood vessel area, both the 2D-UC-MSCs and 3D-UC-MSCs groups showed significantly larger areas compared to the control group (p < 0.05 and p < 0.01, respectively). Again, the 3D-UC-MSC group displayed the most extensive blood vessel area among the groups, with a substantial difference (1.46-fold) when compared to that of 2D-UC-MSCs (Figure 6C). These findings reflect compelling evidence that 3D-UC-MSCs have the capacity to induce enhanced angiogenesis *in vivo*.

4. DISCUSSION

With stem cells emerging as the primary choice for regenerative treatments, cell-based therapy has become a rapidly growing global market. Nonetheless, the therapeutic outcomes vary depending on the source, characteristics, and application areas of these stem cells.[20−22] In the field of regenerative medicine, UC-MSC culture has been a subject of increasing interest.[1,9,23] 3D culture is a cell culture technique that involves growing cells in a 3D environment, and cells are encouraged to grow and interact in a manner that closely resembles their natural environment within tissues and organs. This technique allows cell aggregate, spheroid, or structure formation that mimics the complexity of *in vivo* conditions.[24,25] In this study, a comprehensive investigation was conducted into the culture of UC-MSCs highlighting two fundamentally different methods for growing these cells: one as a monolayer culture (termed 2D-UC-MSCs) and the other as spheroids (referred to as 3D-UC-MSCs). How these two approaches affect secretome and angiogenesis and blood vessel formation process was explored, not only in controlled *in vitro* laboratory conditions but also in the more complex and dynamic *in vivo* environments.

3D cell cultures can be cultivated with or without a supporting scaffold structure. Cells can be cultured in a wide

https://doi.org/10.1021/acsomega.4c02037
ACS Omega 2024, 9, 40358−40367

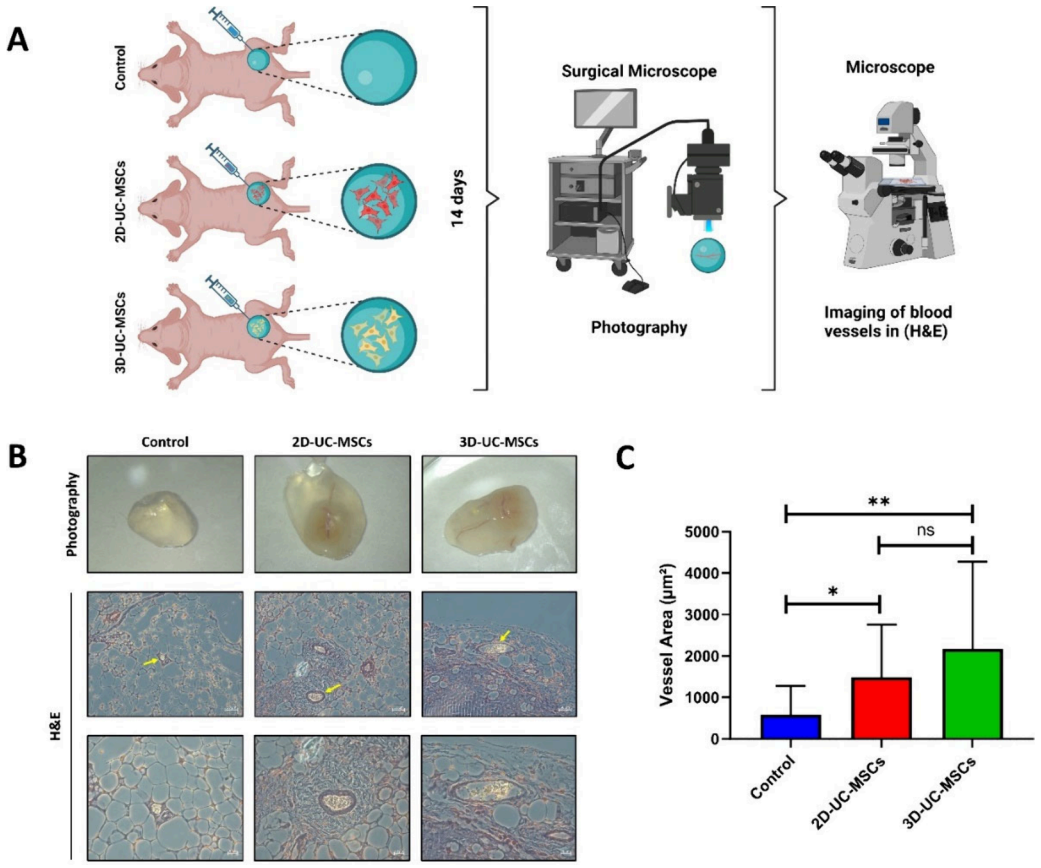

Figure 6. 3D-UC-MSCs and their secretome increased the number of vascular formations in a Matrigel plug mouse model. (A) A schematic illustration of the *in vivo* Matrigel plug mouse model, created using BioRender.com. (B) A representative image and hematoxylin and eosin (H&E) staining of the Matrigel plugs for the control (Matrigel only) and Matrigel +2D-UC-MSCs and Matrigel +3D-UC-MSC groups (n = 6); blood vessels are indicated by yellow arrows (scale bar: 100 and 50 μm). (C) The blood vessel area was determined according to the images obtained from H&E staining. Statistical significance is denoted as follows: *p < 0.05, **p < 0.01 and ns: not significant as determined by the *Student's t test*.

range of cultivation platforms by employing the scaffold method, which encompass solid scaffolds, hydrogels similar to those derived from animal extracellular matrix extracts, proteins, peptides, polymers, and even nanocellulose hydrogels derived from wood, as well as other materials.[26−31] Similarly, 3D cells can be cultured using a variety of methods, including hanging drop plates, nonadherent or U-shaped plates, magnetic levitation, spinner culture, and rotating bioreactors[16,24,32−34] In the present study, a U-shaped microplate (96-well plate) to create a scaffold-free 3D model of UC-MSCs-spheroids was used because scaffold-free 3D cultures more accurately replicate consistent results owing to uniformly sized spheroids, contrary to scaffold 3D cultures as spheroidal size may vary.[35] Additionally, the presence of the scaffold material can introduce variable effects into scaffold-based cultures, potentially interfering with experimental outcomes. Scaffold-free systems decrease such confounding factors, allowing researchers to focus on cell-specific responses.[36,37] The expression of specific stemness markers like CD133, CD166, *NANOG*, *OCT4*, *C-MYC*, and *SOX2* is indicative of stemness, signifying the ability of these cells to maintain their undifferentiated state and undergo differentiation when needed.[38−40] Our results showed that these specific stemness markers increased by the spheroids 3D cultures of UC-MSCs compared to 2D monolayer culture and corroborate previous study.[38]

Recently, many studies elucidated the regenerative therapeutic effects of MSCs due to their secretome (growth factors, cytokines, chemokines, nucleic acids, and EVs).[13,14,41,42] Moreover, majority of the studies centered on the growth factors as their secretome for regenerative/angiogenic effects.[11,34,43] However, in our current study, the detection and expression of proangiogenic miRNAs in the CM of both 2D-UC-MSCs and 3D-UC-MSCs were highlighted. The results suggest distinct differences in miRNA expression levels among the two cultures. The miR-21-5p, miR-126-5p, and miR-130a-3p revealed a significantly higher expression in 3D-UC-MSC-CMs compared to that in 2D-UC-MSC-CMs. A recent study showed that miR-21-5p leads to PTEN inhibition, activating the PI3K/p-Akt signaling pathway in endothelial cells. This promotes angiogenesis *in vitro* and vessel formation, including adipose regeneration *in vivo* within fat implants.[44] Another study used an injectable hydrogel with mesoporous silica nanoparticles for the microRNA-21-5p delivery. They attained improved angiogenesis to enhance myocardial infarction therapy in pigs.[45] miR-126-5p enhances endothelial proliferation and mitigates atherosclerosis via Dlk1 inhibition; the increase in miR-126-5p expression in the temporal muscle can promote angiogenesis in chronically ischemic brains of rats.[46,47] The miR-130a shown to control angiogenesis via reduction of the expression of antiangiogenic homeobox genes GAX and HOXA5,[48] our results showed that 3D-UC-MSC-CMs are expressed more in miR-130a compared to 2D-UC-MSC-CMs, which is known to promote angiogenesis.[48−50] Conversely, miR-494-5p was significantly lower in 3D-UC-

https://doi.org/10.1021/acsomega.4c02037
ACS Omega 2024, 9, 40358−40367

MSC-CMs, and miR-494-3p showed improvement in angiogenesis in the *in vitro* and *in vivo* mouse model of myocardial infarction.[51] Notably, miR-204-5p and miR-210-3p were exclusively detected in 3D-UC-MSC-CMs, which are also known to promote angiogenesis.[52−55] These miRNAs may be found in free form in CMs or in EVs present in CMs as enriched levels of miRNAs are present in EVs by protecting miRNA from degradation.[15,56] These findings underscore the significance of the 3D culture method in the enhancement of the specific angiogenic miRNA expression.

The hallmark features of angiogenesis include the activation of endothelial cells, encompassing processes such as proliferation, migration, and tube formation.[57,58] In the present study, both 2D-UC-MSC-CMs and 3D-UC-MSC-CMs were noted to promote endothelial cell proliferation and migration. However, 3D-UC-MSC-CMs showed a significantly higher level of both proliferation and migration compared to their 2D counterparts, which concurs with previous studies.[34,59] Moreover, the study examined the impact of CM from 2D-UC-MSCs and 3D-UC-MSCs on endothelial cell tube formation, which is a crucial process in angiogenesis. The results revealed that 3D-UC-MSC-CMs remarkably increased various parameters related to tube formation, such as total vessel length, number of junctions, and junction density, which concurs with earlier research.[34,59,60] These enhanced angiogenic effects may be attributed to the presence of enriched amount of angiogenic miRNAs[44−47,49,52,55] in 3D-UC-MSC-CMs. This outcome underscores the potential therapeutic benefits of using CM from 3D-cultured UC-MSCs to promote angiogenesis, making it a promising option for regenerative medicine applications. The study not only analyzed the *in vitro* results but also extended into an *in vivo* mouse model. The Matrigel assay have been used to evaluate angiogenetic effects.[50,61,62] Matrigel plugs combined with 2D-UC-MSCs and 3D-UC-MSCs demonstrated remarkable differences in the vascular formation in this study. The 3D-UC-MSC group exhibited more extensive blood vessel area, signifying their capacity to trigger enhanced angiogenesis *in vivo*. These findings underline the translational potential of 3D-UC-MSCs for *in vivo* regenerative therapies.

In our current study, in addition to the proangiogenic miRNAs that were elucidated, it is possible that other proteins, miRNA, or a combination of these factors plays a role in initiating angiogenesis in endothelial cells. Furthermore, to gain a deeper understanding of the specific proangiogenic miRNAs involved in 3D-UC-MSC-mediated angiogenesis, conducting experiments that involve the knockdown and overexpression of these miRNAs is crucial.

5. CONCLUSION

The successful culture of UC-MSCs in both 2D monolayer and 3D spheroid configurations has noteworthy implications for regenerative medicine. The distinct expression of angiogenic miRNAs (miR-21-5p, miR-126-5p, and miR-130a-3p) and enhanced functional effects of 3D-UC-MSCs render them promising candidates for various therapeutic applications. Evidence from *in vitro* and *in vivo* studies emphasizes the superiority of 3D-UC-MSCs in angiogenesis promotion, further highlighting their potential in the field of regenerative medicine.

■ ASSOCIATED CONTENT

Data Availability Statement

The data that support the findings of this study data is available throughout the manuscript and supporting files.

Supporting Information

The Supporting Information is available free of charge at https://pubs.acs.org/doi/10.1021/acsomega.4c02037.

Angiogenic miRNA expression in conditioned media of 2D-UC-MSCs and 3D-UC-MSCs, primers used for real-time PCR (PDF)

■ AUTHOR INFORMATION

Corresponding Author

Byeong-Cheol Ahn − *Department of Nuclear Medicine, School of Medicine, Kyungpook National University, Daegu 41944, Korea; BK21 FOUR KNU Convergence Educational Program of Biomedical Sciences for Creative Future Talents, Department of Biomedical Science, School of Medicine, Kyungpook National University, Daegu 41944, Korea; Department of Nuclear Medicine, Kyungpook National University Hospital, Daegu 41944, Korea;* orcid.org/0000-0001-7700-3929; Phone: 82-53-420-5583; Email: abc2000@knu.ac.kr; Fax: 82-53-200-6447

Authors

Ramya Lakshmi Rajendran − *Department of Nuclear Medicine, School of Medicine, Kyungpook National University, Daegu 41944, Korea*

Prakash Gangadaran − *Department of Nuclear Medicine, School of Medicine, Kyungpook National University, Daegu 41944, Korea; BK21 FOUR KNU Convergence Educational Program of Biomedical Sciences for Creative Future Talents, Department of Biomedical Science, School of Medicine, Kyungpook National University, Daegu 41944, Korea*

Ji Min Oh − *Department of Nuclear Medicine, School of Medicine, Kyungpook National University, Daegu 41944, Korea*

Chae Moon Hong − *Department of Nuclear Medicine, School of Medicine, Kyungpook National University, Daegu 41944, Korea; Department of Nuclear Medicine, Kyungpook National University Hospital, Daegu 41944, Korea*

Complete contact information is available at: https://pubs.acs.org/10.1021/acsomega.4c02037

Author Contributions

R.L.R. and P.G. contributed equally to this study, designed the methodology, were involved in formal analysis, wrote the original draft of the manuscript, and acquired the funding. R.L.R., P.G., and B.C.A. conceptualized the study. R.L.R., P.G., and J.M.O. investigated the study. B.C.A. supervised the study. C.M.H. and B.C.A. validated the study. R.L.R., P.G., J.M.O., C.M.H., and B.C.A. wrote, reviewed, and edited the manuscript. All authors reviewed the manuscript.

Funding

This research was supported by Basic Science Research Program through the National Research Foundation of Korea (NRF) funded by the Ministry of Education (NRF-2021R1I1A1A01040732 and NRF-2022R1I1A1A01068652)

Notes

The authors declare no competing financial interest.

■ ACKNOWLEDGMENTS

Graphics in figures were created with BioRender.com.

■ REFERENCES

(1) Brown, C.; McKee, C.; Bakshi, S.; Walker, K.; Hakman, E.; Halassy, S.; Svinarich, D.; Dodds, R.; Govind, C. K.; Chaudhry, G. R. Mesenchymal Stem Cells: Cell Therapy and Regeneration Potential. *J. Tissue Eng. Regen Med.* **2019**, *13* (9), 1738−1755.
(2) Prajwal, G. S.; Jeyaraman, N.; Kanth V, K.; Jeyaraman, M.; Muthu, S.; Rajendran, S. N. S.; Rajendran, R. L.; Khanna, M.; Oh, E. J.; Choi, K. Y.; Chung, H. Y.; Ahn, B.-C.; Gangadaran, P. Lineage Differentiation Potential of Different Sources of Mesenchymal Stem Cells for Osteoarthritis Knee. *Pharmaceuticals (Basel)* **2022**, *15* (4), 386.
(3) Anudeep, T. C.; Jeyaraman, M.; Muthu, S.; Rajendran, R. L.; Gangadaran, P.; Mishra, P. C.; Sharma, S.; Jha, S. K.; Ahn, B.-C. Advancing Regenerative Cellular Therapies in Non-Scarring Alopecia. *Pharmaceutics* **2022**, *14* (3), 612.
(4) Baksh, D.; Yao, R.; Tuan, R. S. Comparison of Proliferative and Multilineage Differentiation Potential of Human Mesenchymal Stem Cells Derived from Umbilical Cord and Bone Marrow. *Stem Cells* **2007**, *25* (6), 1384−1392.
(5) Yea, J.-H.; Kim, Y.; Jo, C. H. Comparison of Mesenchymal Stem Cells from Bone Marrow, Umbilical Cord Blood, and Umbilical Cord Tissue in Regeneration of a Full-Thickness Tendon Defect in Vitro and in Vivo. *Biochem Biophys Rep* **2023**, *34*, 101486.
(6) Tai, L.; Saffery, N. S.; Chin, S. P.; Cheong, S. K. Secretome Profile of TNF-α-Induced Human Umbilical Cord Mesenchymal Stem Cells Unveils Biological Processes Relevant to Skin Wound Healing. *Regenerative Medicine* **2023**, *18*, 839.
(7) Jensen, C.; Teng, Y. Is It Time to Start Transitioning From 2D to 3D Cell Culture? *Front. Mol. Biosci.* **2020**, *7*, 00033.
(8) Yen, B. L.; Hsieh, C.-C.; Hsu, P.-J.; Chang, C.-C.; Wang, L.-T.; Yen, M.-L. Three-Dimensional Spheroid Culture of Human Mesenchymal Stem Cells: Offering Therapeutic Advantages and In Vitro Glimpses of the In Vivo State. *Stem Cells Transl Med.* **2023**, *12* (5), 235−244.
(9) Colicchia, M.; Jones, D. A.; Beirne, A.-M.; Hussain, M.; Weeraman, D.; Rathod, K.; Veerapen, J.; Lowdell, M.; Mathur, A. Umbilical Cord-Derived Mesenchymal Stromal Cells in Cardiovascular Disease: Review of Preclinical and Clinical Data. *Cytotherapy* **2019**, *21* (10), 1007−1018.
(10) Sart, S.; Tsai, A.-C.; Li, Y.; Ma, T. Three-Dimensional Aggregates of Mesenchymal Stem Cells: Cellular Mechanisms, Biological Properties, and Applications. *Tissue Eng. Part B Rev.* **2014**, *20* (5), 365−380.
(11) Peshkova, M.; Korneev, A.; Suleimanov, S.; Vlasova, I. I.; Svistunov, A.; Kosheleva, N.; Timashev, P. MSCs' Conditioned Media Cytokine and Growth Factor Profiles and Their Impact on Macrophage Polarization. *Stem Cell Research & Therapy* **2023**, *14* (1), 142.
(12) Műzes, G.; Sipos, F. Mesenchymal Stem Cell-Derived Secretome: A Potential Therapeutic Option for Autoimmune and Immune-Mediated Inflammatory Diseases. *Cells* **2022**, *11* (15), 2300.
(13) Glynn, C. L.; Khan, S.; Kerin, M. J.; Dwyer, R. M. Isolation of Secreted microRNAs (miRNAs) from Cell-Conditioned Media. *MIRNA* **2013**, *2* (1), 14−19.
(14) Van den Brande, S.; Gijbels, M.; Wynant, N.; Santos, D.; Mingels, L.; Gansemans, Y.; Van Nieuwerburgh, F.; Vanden Broeck, J. The Presence of Extracellular microRNAs in the Media of Cultured Drosophila Cells. *Sci. Rep* **2018**, *8*, 17312.
(15) Hawke, D. C.; Ahmed, D. B.; Watson, A. J.; Betts, D. H. Murine Blastocysts Release Mature MicroRNAs Into Culture Media That Reflect Developmental Status. *Front Genet* **2021**, *12*, 655882.
(16) Merimi, M.; El-Majzoub, R.; Lagneaux, L.; Moussa Agha, D.; Bouhtit, F.; Meuleman, N.; Fahmi, H.; Lewalle, P.; Fayyad-Kazan, M.; Najar, M. The Therapeutic Potential of Mesenchymal Stromal Cells for Regenerative Medicine: Current Knowledge and Future Understandings. *Front. Cell Dev. Biol.* **2021**, *9*, 661532.
(17) Rao, X.; Huang, X.; Zhou, Z.; Lin, X. An Improvement of the 2̂(-Delta Delta CT) Method for Quantitative Real-Time Polymerase Chain Reaction Data Analysis. *Biostat., Bioinf., Biomath.* **2013**, *3* (3), 71−85.
(18) Justus, C. R.; Leffler, N.; Ruiz-Echevarria, M.; Yang, L. V. In Vitro Cell Migration and Invasion Assays. *J. Vis Exp* **2014**, No. 88, 51046.
(19) Zudaire, E.; Gambardella, L.; Kurcz, C.; Vermeren, S. A Computational Tool for Quantitative Analysis of Vascular Networks. *PLoS One* **2011**, *6* (11), No. e27385.
(20) Mousaei Ghasroldasht, M.; Seok, J.; Park, H.-S.; Liakath Ali, F. B.; Al-Hendy, A. Stem Cell Therapy: From Idea to Clinical Practice. *Int. J. Mol. Sci.* **2022**, *23* (5), 2850.
(21) Zakrzewski, W.; Dobrzyński, M.; Szymonowicz, M.; Rybak, Z. Stem Cells: Past, Present, and Future. *Stem Cell Research & Therapy* **2019**, *10* (1), 68.
(22) Jovic, D.; Yu, Y.; Wang, D.; Wang, K.; Li, H.; Xu, F.; Liu, C.; Liu, J.; Luo, Y. A Brief Overview of Global Trends in MSC-Based Cell Therapy. *Stem Cell Rev. Rep* **2022**, *18* (5), 1525−1545.
(23) Jeyaraman, M.; Rajendran, R. L.; Muthu, S.; Jeyaraman, N.; Sharma, S.; Jha, S. K.; Muthukanagaraj, P.; Hong, C. M.; Furtado da Fonseca, L.; Santos Duarte Lana, J. F.; Ahn, B.-C.; Gangadaran, P. An Update on Stem Cell and Stem Cell-Derived Extracellular Vesicle-Based Therapy in the Management of Alzheimer's Disease. *Heliyon* **2023**, *9* (7), No. e17808.
(24) Urzì, O.; Gasparro, R.; Costanzo, E.; De Luca, A.; Giavaresi, G.; Fontana, S.; Alessandro, R. Three-Dimensional Cell Cultures: The Bridge between In Vitro and In Vivo Models. *Int. J. Mol. Sci.* **2023**, *24* (15), 12046.
(25) Shah, D. D.; Raghani, N. R.; Chorawala, M. R.; Singh, S.; Prajapati, B. G. Harnessing Three-Dimensional (3D) Cell Culture Models for Pulmonary Infections: State of the Art and Future Directions. *Naunyn-Schmiedeberg's Arch. Pharmacol.* **2023**, *396* (11), 2861−2880.
(26) Afewerki, S.; Sheikhi, A.; Kannan, S.; Ahadian, S.; Khademhosseini, A. Gelatin-polysaccharide Composite Scaffolds for 3D Cell Culture and Tissue Engineering: Towards Natural Therapeutics. *Bioeng Transl Med.* **2019**, *4* (1), 96−115.
(27) Bomkamp, C.; Skaalure, S. C.; Fernando, G. F.; Ben-Arye, T.; Swartz, E. W.; Specht, E. A. Scaffolding Biomaterials for 3D Cultivated Meat: Prospects and Challenges. *Adv. Sci. (Weinh)* **2022**, *9* (3), 2102908.
(28) Del Valle, L. J.; Díaz, A.; Puiggalí, J. Hydrogels for Biomedical Applications: Cellulose, Chitosan, and Protein/Peptide Derivatives. *Gels* **2017**, *3* (3), 27.
(29) Fan, D.; Staufer, U.; Accardo, A. Engineered 3D Polymer and Hydrogel Microenvironments for Cell Culture Applications. *Bioengineering* **2019**, *6* (4), 113.
(30) Das, A.; Ringu, T.; Ghosh, S.; Pramanik, N. A Comprehensive Review on Recent Advances in Preparation, Physicochemical Characterization, and Bioengineering Applications of Biopolymers. *Polym. Bull.* **2023**, *80* (7), 7247−7312.
(31) Langhans, S. A. Three-Dimensional in Vitro Cell Culture Models in Drug Discovery and Drug Repositioning. *Front. Pharmacol.* **2018**, *9*, 00006.
(32) Ryu, N.-E.; Lee, S.-H.; Park, H. Spheroid Culture System Methods and Applications for Mesenchymal Stem Cells. *Cells* **2019**, *8* (12), 1620.
(33) Temple, J.; Velliou, E.; Shehata, M.; Lévy, R.; Gupta, P. Current Strategies with Implementation of Three-Dimensional Cell Culture: The Challenge of Quantification. *Interface Focus* **2022**, *12* (5), 20220019.
(34) Gangadaran, P.; Oh, E. J.; Rajendran, R. L.; Oh, J. M.; Kim, H. M.; Kwak, S.; Chung, H. Y.; Lee, J.; Ahn, B.-C.; Hong, C. M. Three-Dimensional Culture Conditioned Bone Marrow MSC Secretome Accelerates Wound Healing in a Burn Injury Mouse Model. *Biochem. Biophys. Res. Commun.* **2023**, *673*, 87−95.

https://doi.org/10.1021/acsomega.4c02037
ACS Omega 2024, 9, 40358−40367

(35) Ajjarapu, S. M.; Tiwari, A.; Kumar, S. Applications and Utility of Three-Dimensional In Vitro Cell Culture for Therapeutics. *Future Pharmacology* **2023**, *3* (1), 213−228.
(36) Alghuwainem, A.; Alshareeda, A. T.; Alsowayan, B. Scaffold-Free 3-D Cell Sheet Technique Bridges the Gap between 2-D Cell Culture and Animal Models. *Int. J. Mol. Sci.* **2019**, *20* (19), 4926.
(37) Anthon, S. G.; Valente, K. P. Vascularization Strategies in 3D Cell Culture Models: From Scaffold-Free Models to 3D Bioprinting. *International Journal of Molecular Sciences* **2022**, *23* (23), 14582.
(38) Cha, H.-M.; Kim, S.-M.; Choi, Y.-S.; Kim, D.-I. Scaffold-Free Three-Dimensional Culture Systems for Mass Production of Periosteum-Derived Progenitor Cells. *J. Biosci Bioeng* **2015**, *120* (2), 218−222.
(39) Brinkhof, B.; Zhang, B.; Cui, Z.; Ye, H.; Wang, H. ALCAM (CD166) as a Gene Expression Marker for Human Mesenchymal Stromal Cell Characterisation. *Gene* **2020**, *763*, 100031.
(40) Tondreau, T.; Meuleman, N.; Delforge, A.; Dejeneffe, M.; Leroy, R.; Massy, M.; Mortier, C.; Bron, D.; Lagneaux, L. Mesenchymal Stem Cells Derived from CD133-Positive Cells in Mobilized Peripheral Blood and Cord Blood: Proliferation, Oct4 Expression, and Plasticity. *Stem Cells* **2005**, *23* (8), 1105−1112.
(41) Bian, D.; Wu, Y.; Song, G.; Azizi, R.; Zamani, A. The Application of Mesenchymal Stromal Cells (MSCs) and Their Derivative Exosome in Skin Wound Healing: A Comprehensive Review. *Stem Cell Res. Ther* **2022**, *13*, 24.
(42) Dabrowska, S.; Andrzejewska, A.; Janowski, M.; Lukomska, B. Immunomodulatory and Regenerative Effects of Mesenchymal Stem Cells and Extracellular Vesicles: Therapeutic Outlook for Inflammatory and Degenerative Diseases. *Front Immunol* **2021**, *11*, 591065.
(43) Gupta, P. K.; Bhat, S.; Kannan, S.; Seetharam, R. N.; Kolkundkar, U. Therapeutic Approach for Hair Growth and Regeneration Using Bioactive Formulation Containing Mesenchymal Stromal Cell-Derived Conditioned Medium. *Journal of Cosmetics, Dermatological Sciences and Applications* **2023**, *13* (3), 182−208.
(44) Sun, D.; Mou, S.; Chen, L.; Yang, J.; Wang, R.; Zhong, A.; Wang, W.; Tong, J.; Wang, Z.; Sun, J. High Yield Engineered Nanovesicles from ADSC with Enriched miR-21-5p Promote Angiogenesis in Adipose Tissue Regeneration. *Biomater Res.* **2022**, *26* (1), 83.
(45) Li, Y.; Chen, X.; Jin, R.; Chen, L.; Dang, M.; Cao, H.; Dong, Y.; Cai, B.; Bai, G.; Gooding, J. J.; Liu, S.; Zou, D.; Zhang, Z.; Yang, C. Injectable Hydrogel with MSNs/microRNA-21-5p Delivery Enables Both Immunomodification and Enhanced Angiogenesis for Myocardial Infarction Therapy in Pigs. *Science Advances* **2021**, *7* (9), No. eabd6740.
(46) Schober, A.; Nazari-Jahantigh, M.; Wei, Y.; Bidzhekov, K.; Gremse, F.; Grommes, J.; Megens, R. T. A.; Heyll, K.; Noels, H.; Hristov, M.; Wang, S.; Kiessling, F.; Olson, E. N.; Weber, C. MicroRNA-126-5p Promotes Endothelial Proliferation and Limits Atherosclerosis by Suppressing Dlk1. *Nat. Med.* **2014**, *20* (4), 368−376.
(47) Chen, C.; Ling, C.; Gong, J.; Li, C.; Zhang, L.; Gao, S.; Li, Z.; Huang, T.; Wang, H.; Guo, Y. Increasing the Expression of microRNA-126-5p in the Temporal Muscle Can. Promote Angiogenesis in the Chronically Ischemic Brains of Rats Subjected to Two-Vessel Occlusion plus Encephalo-Myo-Synangiosis. *Aging (Albany NY)* **2020**, *12* (13), 13234−13254.
(48) Chen, Y.; Gorski, D. H. Regulation of Angiogenesis through a microRNA (miR-130a) That down-Regulates Antiangiogenic Homeobox Genes GAX and HOXA5. *Blood* **2008**, *111* (3), 1217−1226.
(49) Guduric-Fuchs, J.; Pedrini, E.; Lechner, J.; Chambers, S. E. J.; O'Neill, C. L.; Mendes Lopes de Melo, J.; Pathak, V.; Church, R. H.; McKeown, S.; Bojdo, J.; Mcloughlin, K. J.; Stitt, A. W.; Medina, R. J. miR-130a Activates the VEGFR2/STAT3/HIF1α Axis to Potentiate the Vasoregenerative Capacity of Endothelial Colony-Forming Cells in Hypoxia. *Mol. Ther Nucleic Acids* **2021**, *23*, 968−981.
(50) Gangadaran, P.; Rajendran, R. L.; Oh, J. M.; Oh, E. J.; Hong, C. M.; Chung, H. Y.; Lee, J.; Ahn, B.-C. Identification of Angiogenic Cargo in Extracellular Vesicles Secreted from Human Adipose Tissue-Derived Stem Cells and Induction of Angiogenesis In Vitro and In Vivo. *Pharmaceutics* **2021**, *13* (4), 495.
(51) Liu, H.; Zhang, Y.; Yuan, J.; Gao, W.; Zhong, X.; Yao, K.; Lin, L.; Ge, J. Dendritic Cell-Derived Exosomal miR-494-3p Promotes Angiogenesis Following Myocardial Infarction. *Int. J. Mol. Med.* **2020**, *47* (1), 315−325.
(52) Ding, M.; Chi, G.; Li, F.; Wang, B.; Shao, C.; Song, W. Up-Regulated miR-204-5p Promoted the Migration, Invasion, and Angiogenesis of Endothelial Progenitor Cells to Enhance the Thrombolysis of Rats with Deep Venous Thrombosis by Targeting SPRED1. *Exp. Cell Res.* **2022**, *411* (1), 112985.
(53) Tiwari, A.; Mukherjee, B.; Dixit, M. MicroRNA Key to Angiogenesis Regulation: MiRNA Biology and Therapy. *Curr. Cancer Drug Targets* **2018**, *18* (3), 266−277.
(54) Landskroner-Eiger, S.; Moneke, I.; Sessa, W. C. miRNAs as Modulators of Angiogenesis. *Cold Spring Harb Perspect Med.* **2013**, *3* (2), a006643.
(55) Wei, S.; Qiu, Y. MiR-210-5p Regulates STAT3 Activation by Targeting STAT5A in the Differentiation of Dermal Fibroblasts. *3 Biotech* **2021**, *11* (5), 243.
(56) Endzeliņš, E.; Berger, A.; Melne, V.; Bajo-Santos, C.; Soboļevska, K.; Ābols, A.; Rodriguez, M.; Šantare, D.; Rudņickiha, A.; Lietuvietis, V.; Llorente, A.; Linē, A. Detection of Circulating miRNAs: Comparative Analysis of Extracellular Vesicle-Incorporated miRNAs and Cell-Free miRNAs in Whole Plasma of Prostate Cancer Patients. *BMC Cancer* **2017**, *17* (1), 730.
(57) Yan, Y.; Song, Q.; Yao, L.; Zhao, L.; Cai, H. YAP Overexpression in Breast Cancer Cells Promotes Angiogenesis through Activating YAP Signaling in Vascular Endothelial Cells. *Anal. Cell Pathol.* **2022**, *2022*, 5942379.
(58) Saman, H.; Raza, S. S.; Uddin, S.; Rasul, K. Inducing Angiogenesis, a Key Step in Cancer Vascularization, and Treatment Approaches. *Cancers (Basel)* **2020**, *12* (5), 1172.
(59) Caneparo, C.; Baratange, C.; Chabaud, S.; Bolduc, S. Conditioned Medium Produced by Fibroblasts Cultured in Low Oxygen Pressure Allows the Formation of Highly Structured Capillary-like Networks in Fibrin Gels. *Sci. Rep* **2020**, *10* (1), 9291.
(60) Chae, D.-S.; An, S. J.; Han, S.; Kim, S.-W. Synergistic Therapeutic Potential of Dual 3D Mesenchymal Stem Cell Therapy in an Ischemic Hind Limb Mouse Model. *International Journal of Molecular Sciences* **2023**, *24* (19), 14620.
(61) Chander, S. K.; Foster, P. A.; Leese, M. P.; Newman, S. P.; Potter, B. V. L.; Purohit, A.; Reed, M. J. In Vivo Inhibition of Angiogenesis by Sulphamoylated Derivatives of 2-Methoxyoestradiol. *Br. J. Cancer* **2007**, *96* (9), 1368−1376.
(62) Gangadaran, P.; Rajendran, R. L.; Oh, J. M.; Hong, C. M.; Jeong, S. Y.; Lee, S.-W.; Lee, J.; Ahn, B.-C. Extracellular Vesicles Derived from Macrophage Promote Angiogenesis In Vitro and Accelerate New Vasculature Formation In Vivo. *Exp. Cell Res.* **2020**, *394* (2), 112146.

https://doi.org/10.1021/acsomega.4c02037
ACS Omega 2024, 9, 40358−40367